Structural and Multidisciplinary Optimization (2020) 62:1117–1133
https://doi.org/10.1007/s00158-020-02542-2

RESEARCH PAPER

A multi-objective optimization of the friction stir welding process using RSM-based-desirability function approach for joining aluminum alloy 6063-T6 pipes

S. M. Senthil[1] · R. Parameshwaran[2] · S. Ragu Nathan[3] · M. Bhuvanesh Kumar[1] · K. Deepandurai[1]

Received: 10 October 2019 / Revised: 8 December 2019 / Accepted: 10 February 2020 / Published online: 3 March 2020

Abstract

In this study, a multi-objective optimization technique involving response surface methodology (RSM)-based desirability function approach is used in optimizing the process parameters for friction stir welding of AA6063-T6 pipes. Two process parameters, namely, tool rotational speed and weld speed, are optimized for achieving a weld joint having superior tensile properties, viz., maximum yield, and ultimate tensile strength and maximum % of elongation. A regression model, with a 95% confidence level, is developed using response surface methodology to predict the tensile strength of the weld joint. ANOVA technique is used to determine the adequacy of the developed model and identify the significant terms. The desirability function is used to analyze the responses and predict the optimal process parameters. It is found that tool rotational speed and weld speed have equal influence over the tensile strength of the pipe weld. Tool rotational speed 1986 rpm and weld speed 0.65 rpm have yielded a maximum ultimate tensile strength of 167 MPa, yield strength of 145 MPa, and % elongation of 8.3, under considered operating conditions. Microstructural attributes for superior weld properties are also discussed.

Keywords Aluminum pipe · FSW · Optimization · RSM · Desirability function · Tensile strength

1 Introduction

Joining pipes using friction stir welding (FSW) process is taking shape from the laboratory research level. The delivery of high weld strength is one of the significant advantages of the FSW process, whose choices and ranges are being exploited through rigorous research activities since its inception. Pipe joining technology usually involves fusion welding techniques in which many distortions take place, making it prone to defects/failures. Now, researchers are working for the replacement of fusion welding techniques by the FSW process to make use of its advantages. Like other welding processes, FSW also has a quite number of process parameters controlling the quality of the weld. Extensive works have been carried out in understanding the effect of process parameters on the welding of plat plates. The primary choice of factors for FSW process optimization includes tool design (pin profile and tool shoulder diameter), tool rotational speed, and weld speed. Padmanaban and Balasubramanian (Padmanaban and Balasubramanian 2009) optimized the tool characteristics namely, pin profile, shoulder diameter, and tool material for FSW of AZ31B magnesium alloy. Commin et al. (Commin et al. 2009) performed FSW of AZ31 magnesium alloy and found that the heat generation increased due to the increase in shoulder diameter and tool rotational speed, whereas the increase in weld speed decreased the heat generation in the weld zone. Vijay and Murugan (Vijay and Murugan 2010), after performing an investigation in FSW of Al–10 wt% TiB_2 metal matrix composite concluded that straight square pin profiles produced high strength joints. Chouhan et al. (Chouhan et al. 2013) found that maximum tensile strength in FSW of flat plate 6063 aluminum alloy can be produced at an optimized value of tool rotational speed of 562 rpm and weld speed of 23 mm/

Responsible Editor: Ren-Jye Yang

✉ S. M. Senthil
senthil.awaits@gmail.com

[1] Department of Mechanical Engineering, Kongu Engineering College, Erode, India

[2] Department of Mechatronics Engineering, Kongu Engineering College, Erode, India

[3] Micromachining Research Centre (MMRC), Department of Mechanical Engineering, Sree Vidyanikethan Engineering College, Tirupati, India

min. Other factors like axial load, tool tilt angle, and preheating conditions also show up in the factors list. Effect of tilt angle was studied by Mehta and Badheka (Mehta and Badheka 2016) during FSW of copper to aluminum, and they found that its effect is significant for dissimilar joints fabrication. Also, the effects of axial load and tool torques were studied by Su et al. (Su et al. 2013) for FSW of AA2024-T4 aluminum alloys. Many such works can be found in the literature supporting the fact that flat plate geometries are well established. However, when it comes to FSW of pipes, only a few works have been carried out so far in understating the effects of process parameters. Doos (Doos 2012) employed FSW for joining 6061-T6 aluminum pipes and studied the effect of process parameters on the weldment. Lammlein et al. (Lammlein et al. 2012) performed an experimental and numerical study on the joining of 6061-T6 aluminum alloy pipes. They recommended that high traverse speed could increase the process viability. Khourshid and Sabry (Khourshid and Sabry 2013) studied the effect of process parameters on FSW of 6063 aluminum alloy and reported that both tool rotational speed and weld speed had a combined effect on the weld joint efficiency. Ismail et al. (Ismail et al. 2013) performed full penetration FSW of 6063 aluminum pipes and concluded that high tool rotational speed of 1500 rpm and weld speed of 144 mm/min gave defect-free welds. Even though these works try to portray the effects of process parameters, they lack the optimal results. None of the studies have used proper tools/methods to optimize the process parameters.

However, optimization of the FSW process parameters using proper tools/techniques has yielded good optimal results, which is a proven datum for flat plate geometries. Most of these optimization studies are aimed at improving the tensile strength of the welded joint, which is one of the vital advantages while using the FSW process. Widely used techniques are the Taguchi method and response surface methodology (RSM). Bayazid et al. (Bayazid et al. 2015) employed the Taguchi method for optimizing the process parameters involved in fabricating 6063–7075 aluminum alloys butt joints. Kadaganchi et al. (Kadaganchi et al. 2015) employed RSM for optimizing the process parameters for FSW of AA 2014-T6 plates. Ghaffarpour et al. (Ghaffarpour et al. 2017) employed RSM for FSW of dissimilar 5083-H12 and AA6061-T6 thin sheets, whereas Mallieswaran et al. (Mallieswaran et al. 2018) used RSM for optimizing the process parameters involved in FSW of dissimilar AA1100-AA6061 sheets. Similar other works can also be found in the literature with a wide variety of applications. All these optimizations work, in general, use the Taguchi method and RSM to generate the design matrix. The responses are validated using analysis of variance (ANOVA), which is an essential mathematical procedure.

Other optimization tools include artificial neural networks (ANN), genetic algorithm, grey relational analysis (GRA), and other soft computing techniques that address exclusive application benefits. Adyin (Aydin et al. 2010) studied the feasibility in optimizing the process parameters of FSW of AA1050-H22 aluminum alloy using Taguchi-based GRA method. ANN with GA was used by Babu et al. (Babu et al. 2017) to optimize the cryorolled AA2219 alloy welds. The prediction capability of the design model is critical in achieving an optimal solution. Recent studies are trying to increase this capability by combining traditional techniques with non-traditional techniques. Such multi-objective optimization techniques result in more optimized results than single objective techniques. Sahu et al. (Sahu et al. 2016) employed a hybrid fuzzy-grey-Taguchi-based multi-objective model to optimize the weld quality of the Al/Cu dissimilar friction stir welded joints. In this study, the Taguchi array was used to conduct the experiments, which was then followed by the conversion of multi-level characteristics into single-level characteristics using a fuzzy interface system. Finally, optimization was carried out using the Taguchi method, based on which optimal conditions had arrived. Gupta et al. (Gupta et al. 2018) used a hybrid approach in optimizing the process parameters involved in FSW of dissimilar AA5083/AA6063 aluminum alloys. This hybrid approach uses grey relational analysis with principal component analysis (PCA). The PCA is used here to obtain the weighting factors for each response by converting grey relational coefficients into matrix form. Sudhagar et al. (Sudhagar et al. 2017) employed GRA and Technique for Order Preference by Similarity to Ideal Solution (TOPSIS) decision-making techniques to optimize the process parameters for FSW of aluminum 2024 alloy. Wakchaure et al. (Wakchaure et al. 2018) used a combination of the Taguchi-Grey relation analysis-ANN method to the friction stir welding parameters to join the 6082-T6 aluminum alloy. They have demonstrated the application feasibility of ANN-GRA in combination with Taguchi for improved joint strength.

Only a few works have been carried out using desirability functions to optimize the FSW process parameters by assigning weights to the responses. Desirability functions are usually combined with RSM technique, which helps in predicting more optimal results as like the studies of Srivastava et al. (Srivastava et al. 2017). Verma et al. (Verma et al. 2018) used the desirability approach to optimize the process parameters in FSW of armor-marine grade aluminum alloy. They have used RSM to predict the responses, from which the desirability functions were used to optimize the responses. Pandiyarajan et al. (Pandiyarajan et al. 2019) used the desirability approach to optimize FSW process parameters. He successfully optimized the process parameters for optimal weld strength and nugget hardness of AA 6061-ZrO_2-C composites. Similar works were also carried out in optimizing the milling (Selaimia et al. 2017) and other industrial processes.

The works related to optimization of FSW process for joining aluminum alloy pipes are seldom found. Hence, in this work, a unique attempt has been made to optimize the process parameters for FSW of aluminum pipes. A popular tool used for optimizing the FSW process in joining plates, viz., RSM-based desirability function approach, is employed. The proposed optimization process focuses on deriving a regression model for predicting the tensile strength of the pipe joint. RSM is used to derive the effects of various process parameters over the tensile strength with the help of ANOVA. These effects on the responses are further optimized using desirability functions.

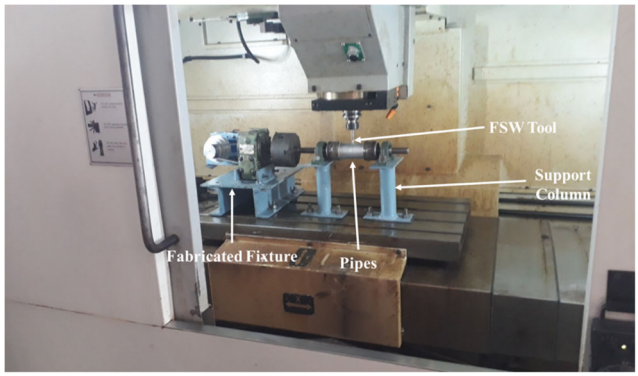

Fig. 1 Developed rotary fixture for friction stir welding of pipe installed within CNC milling center

2 Methods and materials

2.1 Experimental works

The AA6063-T6 pipes with OD 50 mm and thickness 3 mm are used for this study. Chemical composition and mechanical properties of the AA6063-T6 aluminum alloy are given in Table 1. FSW is carried out using a CNC milling center, assisted with an indigenously developed rotary fixture. In this pipe welding, the welding speed is controlled by the developed rotary fixture, which is externally powered and designed to deliver the required speeds. The fixture setup consists of motor arrangements and a reduction gearbox, which delivers the required speed to the chuck. The pipes to be welded are mounted firmly on a specially designed mandrel, which is fixed into the chuck. The mandrel is supported by two support columns to withstand the tool load. The assembled image of the rotary fixture installed within the CNC milling center is shown in Fig. 1.

2.2 Process parameters considered for optimization

Based on literature studies and experimental trials, a cause and effect diagram (Fig. 2) is developed in order to segregate the influential parameters over the tensile strength. Grain structure modification during FSW is highly influenced by heat input. The heat generation during the process can be controlled only by varying the tool rotational speed and welding speed (Ganapathy et al. 2017; Sashank et al. 2018). Hence, tool rotational speed and weld speed are considered for optimization, keeping other parameters as constant. The fixed process parameters are shown in Table 2. Various trials and preliminary experiments were conducted to confine the range for the variable process parameters. The selected range for the variable process parameters is given in Table 3. Figure 3 portrays the weld surfaces obtained from the trial runs performed. Figure 3 a shows the defective welds produced due to insufficient tool rotational speed (less than 1800 rpm) and low weld speed (less than 0.4 rpm). Figure 3 b shows the defective welds obtained due to high tool rotational speed (more than 2200 rpm) and high weld speed (more than 0.6 rpm). Whereas the weld surfaces obtained using parameters inside the selected range are given in Fig. 3 c, they are found to have a smooth weld surface and defect-free.

2.3 Testing and metallurgical studies

After the welding process, the pipe joints are subjected to a radiography test in order to check for internal flaws. Radiography tests are carried out as per ASTM 02A–6. Single-Wall Single-Image (SWSI) technique is used (Fig. 4). Acceptance levels during the evaluation are of radiographic standards ASTM E-466 and ASTM E-186. The tensile test is carried out using the Universal Testing Machine – electronic tensometer as per ASTM E8M-04 standard. The tensile test specimen dimensions are cut using the Wire EDM machine as per the standard. Three specimens from the same pipe weld have been taken at random locations along the weld circumference. Tensile results of these three samples are averaged in order to check and ensure the uniform facilitation offered by the developed fixture throughout the weld. Yield strength (YS), ultimate tensile strength (UTS), and percentage of

Table 1 Chemical composition and mechanical properties of AA6063-T6 aluminum alloy

Chemical composition (wt%)									Mechanical property		
Al	Si	Fe	Cu	Mn	Mg	Cr	Zn	Ti	YS (MPa)	UTS (MPa)	%E
Reminder	0.4	0.35	0.10	0.10	0.60	0.10	0.10	0.10	214	241	12

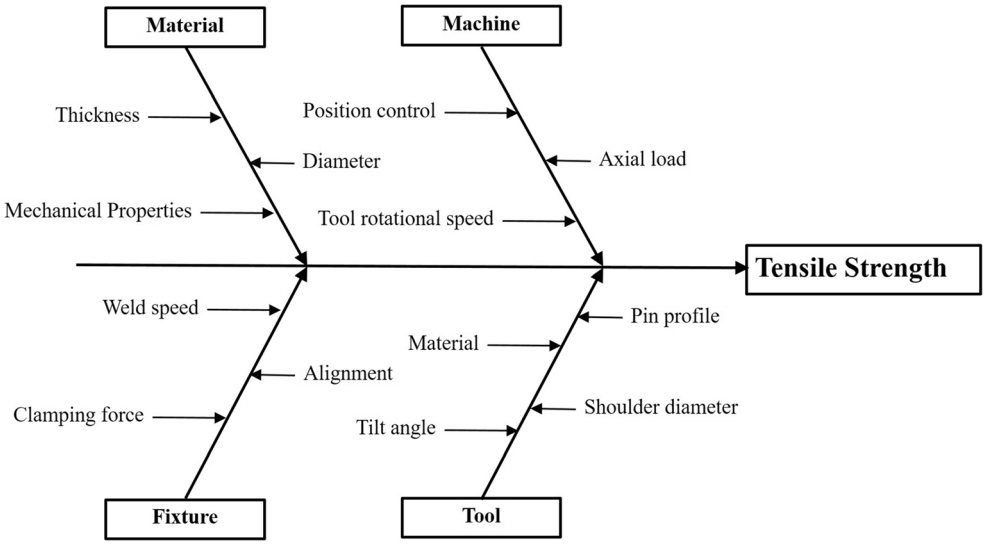

Fig. 2 Cause and effect diagram for tensile strength influencing parameters

elongation (% E) are measured. Microstructure studies are carried out using an inverted metallurgical microscope. The samples are cut along the weld cross-section, and surfaces are prepared using different grades of emery sheets and finally using velvet cloth added with diamond paste. The surface of the samples is etched using Keller's solution for about 20 s to reveal the grain boundaries.

3 Model development

3.1 Response surface methodology

Response surface methodology (RSM) is one of the effective mathematical techniques for analyzing problems in which several variables influence a response. The search of the RSM is to find the maximum of the response. Relationship models between response and variables can be derived, which helps in understanding their influence levels. Geometrical and contour plots can also be obtained, which are visual aids for better appreciation of the relationship behavior. Central composite design (CCD) is employed for this study with full factorial. A total of two factors are considered, namely, tool rotational speed (A) and weld speed (B). The process parameters, along with their working ranges and level indications, are provided in Table 3. Three levels are considered with the upper limit as + 1 and lower limit as − 1, and the star point is the average of − 1 and + 1 values. The alpha value (α) is set to be 1. A total of 13 runs are generated, for which experiments are carried out, and the average response is tabulated in the design matrix Table 4.

In order to predict the responses, a quadratic polynomial equation is developed using this model. This equation predicts the response as a function of independent variables involving their interactions (Kalavathy et al. 2009). In general, the predicted response (Y_i) for a coded independent variable (x_i, x_j) is given by Eq. 1.

$$Y_i = \beta_0 + \sum_i \beta_i x_i + \sum_{ii} \beta_{ii} x_{ii}^2 + \sum_{ij} \beta_{ij} x_i x_j \quad (1)$$

Where β_0 is the coefficient of interception, β_i are the linear terms, β_{ii} are the squared terms, and β_{ij} are the interaction terms. RSM is used to calculate the coefficients of this response model. An academic licensed version of Minitab 2018 software is used to carry out the RSM technique and conduct various statistical studies for validating the model.

3.2 Model adequacy

ANOVA technique is used in developing the adequacy of the model. The ANOVA for yield strength, ultimate tensile

Table 2 Fixed process parameters

S No.	Process parameters	Values
	Tool pin profile	Taper cylindrical
	Axial load	1 kN
	Tool tilt angle	0°
	Tool material	High speed steel

Table 3 Variable process parameters with working ranges

S No.	Process parameters	Levels		
		−1	0	+1
	Tool rotational speed in rpm (A)	1800	2000	2200
	Weld speed in rpm (B)	0.4	0.6	0.8

Defects due to insufficient tool rotational speed (less than 1800rpm) and low weld speed (less than 0.4rpm)

Defects due to high weld speed (more than 2200rpm) and high weld speed (more than 0.6rpm)

Smooth and clear weld surface under the selected process parameter range

Fig. 3 Trial weld images

strength, and % elongation are given in Tables 5, 6, and 7. The adequacy of the developed model is recognized as Tables 5, 6, and 7 indicates the *P* value to be less than the *F* value, under 95% confidence level for all the responses considered. Also, for this developed model with a 95% confidence level, the *P* value is less than 0.05, which makes the developed model significant. Also *R* square value for the YS model is 0.9436 (94.36%), for UTS model is 0.9478 (94.78%), and for %E model is 0.9621 (96.21%). The residual plots for YS, UTS, and %E against the normal probability % are given in Fig. 5. It shows the residuals following a straight line, which confirms the normal distribution of errors. Figure 6 shows the plot between experimental and predicted values, thus confirming the good correlation between them. The above observations in total indicate very good adequacy of the developed model.

The final model is developed after determining all the significant coefficients, for predicting yield strength, ultimate tensile strength, and % elongation of friction stir welded pipe joints of AA6063-T6 aluminum alloy, and is presented in the Eqs. 2, 3, 4. The predicted responses are given in Table 8.

$$\mathrm{YS} = -1576 + 1.695\ \mathrm{A} + 161\ \mathrm{B} - 0.000435\ \mathrm{A*A} - 172.4\ \mathrm{B*B}, + 0.0312\ \mathrm{A*B} \tag{2}$$

$$\mathrm{UTS} = -1922 + 1.969\ \mathrm{A} + 256\ \mathrm{B} - 0.000478\ \mathrm{A*A} - 153.4\ \mathrm{B*B} - 0.0250\ \mathrm{A*B} \tag{3}$$

$$\%\mathrm{E} = -128.9 + 0.1371\ \mathrm{A} + 8.99\ \mathrm{B} - 0.000035\ \mathrm{A*A} - 7.63\ \mathrm{B*B} + 0.00062\ \mathrm{A*B} \tag{4}$$

3.3 Desirability function (DF) approach

The desirability function approach is a method that is used widely for multiple response optimization processes (Myers et al. 2016). This method finds operating conditions *x* that provide the *most desirable* response values. In this approach, all the responses are converted into individual DFs (d_i) having the scale factor between 0 and 1. These functions are structured by setting up the values as the target or minimum or maximum response (y_i) obtained through the experiments (Derringer and Suich 1980). Let *L*, *U,* and *T* be the minimum, target, and maximum values, respectively, which are desired for response *y*, with $L \le T \le U$.

If a response is of the *target is best* kind, then its individual desirability function is

$$d_i = \begin{cases} 0 & y_i < L \\ \left(\frac{y_i - L}{T - L}\right)^r & L \le y_i \le T \\ \left(\frac{U - y_i}{U - T}\right)^s & T \le y_i \le U \\ 0 & y_i > U \end{cases} \tag{5}$$

with the exponents *r* and *s* determining how important it is to hit the target value. For $r = s = 1$, the desirability function increases linearly toward *T*; for $r < 1$, $s < 1$, the function is convex, and for $r > 1$, $s > 1$, the function is concave.

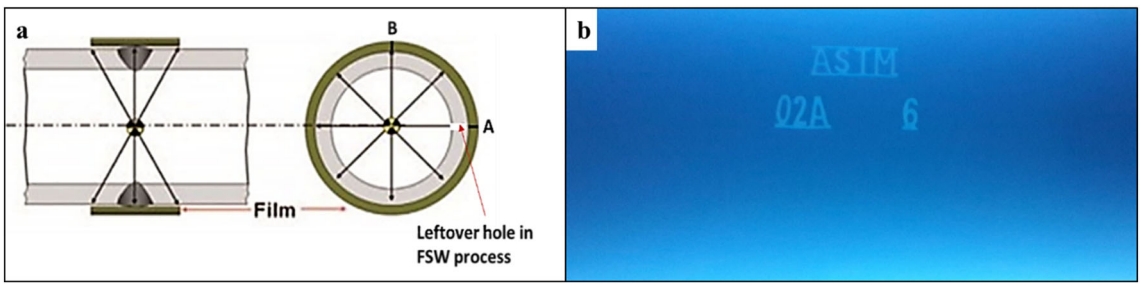

Fig. 4 **a** SWSI technique. **b** Sample image result of radiography test

Table 4 Design matrix and experimental responses

Std order	Run order	Process parameters		Average experimental responses		
		Tool rotational speed (rpm) A	Weld speed (rpm) B	Yield strength (MPa) YS	Ultimate tensile strength (MPa) UTS	% of elongation %E
1	13	1800	0.4	125	132	6.8
2	8	2200	0.4	115	151	5.5
3	3	1800	0.8	130	144	7.3
4	2	2200	0.8	125	159	6.1
5	12	1800	0.6	135	140	7.1
6	7	2200	0.6	119	154	5.9
7	9	2000	0.4	135	157	7.5
8	11	2000	0.8	140	163	7.7
9	6	2000	0.6	150	168	8
10	10	2000	0.6	151	171	7.8
11	1	2000	0.6	145	171	8.1
12	4	2000	0.6	144	175	8.3
13	5	2000	0.6	149	172	8.4

If a response is to be minimized, the individual desirability is defined as:

$$d_i = \begin{cases} 1 & y_i < L \\ \left(\frac{U-y_i}{U-T}\right)^s & T \le y_i \le U \\ 0 & y_i > U \end{cases} \quad (6)$$

with T denoting a small enough value for the response.

If a response is to be maximized instead, the individual desirability is defined as:

$$d_i = \begin{cases} 0 & y_i < L \\ \left(\frac{y_i-L}{T-L}\right)^r & L \le y_i \le T \\ 1 & y_i > T \end{cases} \quad (7)$$

with T, in this case, interpreted as a large enough value for the response.

Table 5 ANOVA for yield strength (YS)

Source	DF	Adj SS	Adj MS	*F* value	*P* value	
Model	5	1659.83	331.967	23.41	0.000	Significant
Linear	2	226.83	113.417	8.00	0.016	
A	1	160.17	160.167	11.30	0.012	
B	1	66.67	66.667	4.70	0.067	
Square	2	1426.75	713.375	50.32	0.000	
A*A	1	835.86	835.863	58.96	0.000	
B*B	1	131.36	131.363	9.27	0.019	
2-Way interaction	1	6.25	6.250	0.44	0.528	
A*B	1	6.25	6.250	0.44	0.528	
Error	7	99.24	14.178			
Lack-of-fit	3	60.44	20.148	2.08	0.246	Not significant
Pure error	4	38.80	9.700			
Total	12	1759.08				
Model summary						
R square		Adjusted *R* square		Predicted *R* square		
94.36%		90.33%		68.35%		

Table 6 ANOVA for ultimate tensile strength (UTS)

Source	DF	Adj SS	Adj MS	*F* value	*P* value	
Model	5	2094.84	418.97	25.40	0.000	Significant
Linear	2	496.67	248.33	15.05	0.003	
A	1	384.00	384.00	23.28	0.002	
B	1	112.67	112.67	6.83	0.035	
Square	2	1594.17	797.08	48.32	0.000	
A*A	1	1011.58	1011.58	61.32	0.000	
B*B	1	104.05	104.05	6.31	0.040	
2-Way interaction	1	4.00	4.00	0.24	0.637	
A*B	1	4.00	4.00	0.24	0.637	
Error	7	115.47	16.50			
Lack-of-fit	3	90.27	30.09	4.78	0.083	Not significant
Pure error	4	25.20	6.30			
Total	12	2210.31				
Model summary						
R square		Adjusted *R* square		Predicted *R* square		
94.78%		91.04%		69.23%		

The individual desirability are then combined using the geometric mean, which gives the *composite desirability D*,

$$D = (d_1, d_2, d_3, \ldots\ldots, d_n)^{\frac{1}{n}} = \left(\prod_{i=1}^{n} d_i\right)^{\frac{1}{n}} \quad (8)$$

The highest possible value of *D* is desired for obtaining the optimal conditions of the responses. For our model, all the responses are to be optimized for the maximum level. The curve shape for the desirability function for maximized responses is given in Fig. 7. In this research work, to determine the optimal values of the input parameters, namely, tool rotational speed (A) and weld speed (B), composite DF is used. The input parameters are optimized for the maximized values of the output responses, namely YS, UTS, and %E.

4 Results and discussion

The developed model is used to evaluate the influence of the process parameters, namely, tool rotational speed and weld speed, on the friction stir welding process of AA6063-T6 pipes. As per the objective of the model, optimal process parameters are found. In the FSW process, the heat source

Table 7 ANOVA for percentage elongation (%E)

Source	DF	Adj SS	Adj MS	*F* value	*P* value	
Model	5	10.3015	2.06029	35.50	0.000	Significant
Linear	2	2.5633	1.28167	22.08	0.001	
A	1	2.2817	2.28167	39.32	0.000	
B	1	0.2817	0.28167	4.85	0.063	
Square	2	7.7356	3.86781	66.65	0.000	
A*A	1	5.4534	5.45341	93.97	0.000	
B*B	1	0.2572	0.25722	4.43	0.073	
2-Way interaction	1	0.0025	0.00250	0.04	0.841	
A*B	1	0.0025	0.00250	0.04	0.841	
Error	7	0.4062	0.05803			
Lack-of-fit	3	0.1782	0.05941	1.04	0.465	Not significant
Pure error	4	0.2280	0.05700			
Total	12	10.7077				
Model summary						
R square		Adjusted *R* square		Predicted *R* square		
96.21%		93.50%		84.24%		

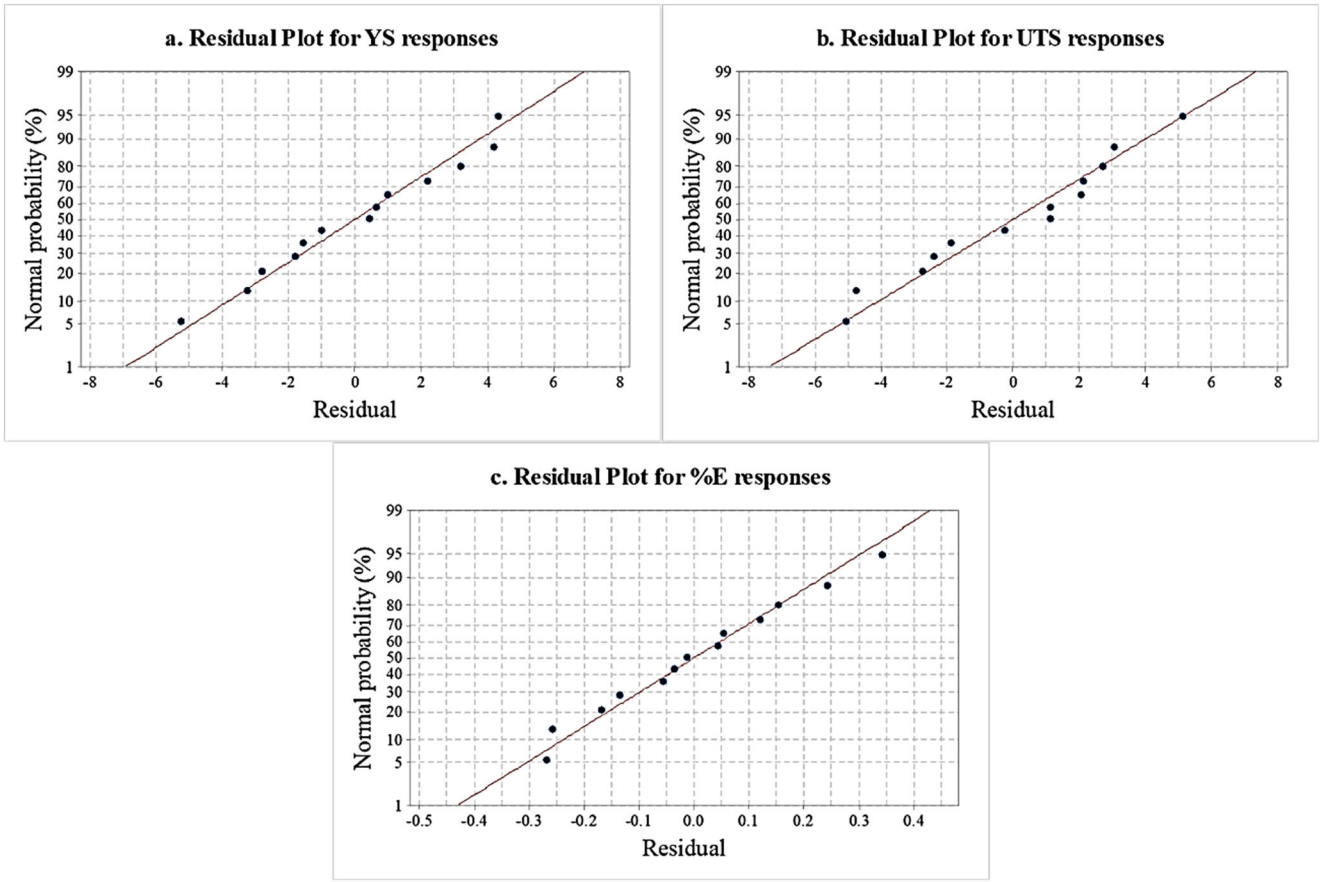

Fig. 5 Normal plots of response residuals

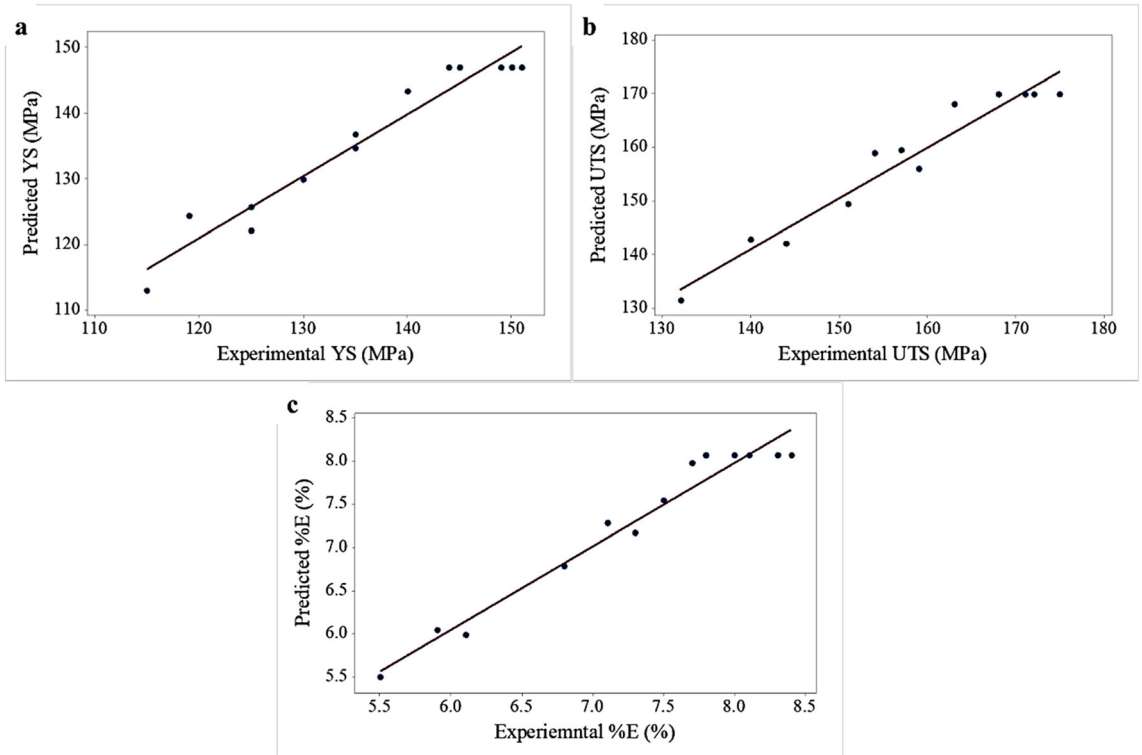

Fig. 6 Experimental vs. predicted values of the response

Table 8 Predicted responses from RSM (after omitting repeated runs)

Run order	Predicted responses		
	YS (MPa)	UTS (MPa)	%E
1	146.83	169.90	8.06
2	121.95	155.95	5.97
3	129.78	141.95	7.16
7	124.26	158.76	6.04
8	112.78	149.29	5.49
9	136.60	159.43	7.54
11	143.26	168.09	7.97
12	134.60	142.76	7.27
13	125.62	131.29	6.77

required for welding is generated through frictional contact between the tool and the workpiece. These process parameters ultimately influence the in-total heat generated at the contacting instant. For the welding system to be considered, i.e., FSW of pipes, weld speed is controlled by a fourth axis rotary unit, which is a retrofit. All the variables considered are independent and have their own influencing limit over the tensile strength (response) of the weld joint. The FSW process is generally associated with three precipitation zones, namely, stir zone (SZ), thermo-mechanically affected zone (TMAZ), and heat affect zone (HAZ), among which SZ and TMAZ where grain zine and boundaries are altered at a larger extent. These SZ and TMAZ account for the loss in the tensile property when compared to that of the base metal. The process variables (parameters), namely, tool rotational speed and weld speed, have a significant influence on these zones, which is evident from the main effects plots Figs. 8, 10, and 12.

4.1 Influence of process parameters on ultimate tensile strength

Figure 8 shows the main effects plot for ultimate tensile. The mean of UTS is low at the extreme levels − 1 and + 1, while it is maximum at the middle level 0. The ultimate tensile strength of the weld increases as the tool rotational speed

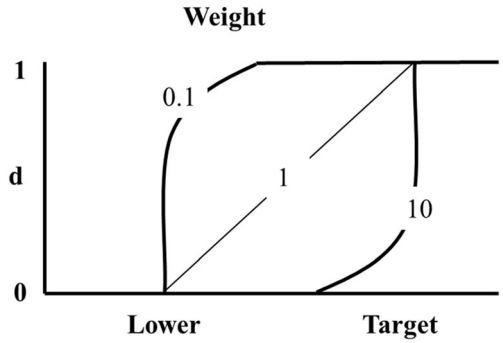

Fig. 7 Curve shape for desirability function with maximization condition

increases to the middle level (2000 rpm) and decreases thereon. At lower speeds, the yield strength decreases to a very much lower value. The welding speed also has a similar effect giving a maximum effect in the middle level (0.6 rpm). Figure 9 shows the contour plot of the combined effect of tool rotational speed and weld speed on the ultimate tensile strength. Usually, heat generation increases with an increase in tool rotational speed and weld speed (Arbegast 2003), which will have more influence on the tensile strength (Elangovan and Balasubramanian 2007; Elangovan and Balasubramanian 2008; Wang et al. 2015). With the combined effect of tool rotational speed and weld speed, the maximum response is concentrated in the central region of the plot, i.e., around the midlevel factors. Tensile strength is lower at tool rotational speeds of 1800 rpm and 2200 rpm and is maximum at 2000 rpm. Also, extreme weld speeds (0.4 rpm and 0.8 rpm) have produced low tensile values, whereas the 0.6 rpm has yielded a higher value of tensile strength. The contour plot for UTS shows an average peak value in tensile strength of 170 MPa. The combined tool and weld speed along with the taper cylindrical tool pin profile have supported in minimizing the formation of Mg_2Si precipitates and in turn, resulted in a higher tensile property (Gadakh and Adepu 2013).

4.2 Influence of process parameters on yield strength

Figure 10 shows the main effects plot between process parameters and yield strength. The influence pattern follows the same as for the ultimate tensile strength. The midlevel of tool rotational speed and weld speed produces maximized yield strength of the weld joint. Higher tool rotational speeds lead to lower yield strength values. Eq. 2 describes the nature of the contribution of process parameters for the yield strength of the weld joint. The negative coefficient of weld speed means, its increase decreases the yield strength. Similarly, the positive coefficient of tool rotational speed directs the increase in yield strength as the rotational speed increases. The yield strength is controlled by the amount of heat generated in the weld zone. This heat generation is majorly influenced by the tool rotational speed and weld speed as per the Arbegast equation (Arbegast 2003) as follows:

$$\text{Heat input, } HI = K\left(\frac{\omega^2}{\vartheta\, x\, 10^4}\right)^{\alpha} \tag{9}$$

where ω is rotational speed, ϑ is the welding speed, and K and α are the material constants. This equation shows that both weld speed and tool rotational speed have an opposite effect on the yield strength, which is evident from Eq. 2. The contour plot (Fig. 11) depicts the combined effect of the tool rotational speed and weld speed on the yield strength of the weld joint. The optimal conditions are concentrated around

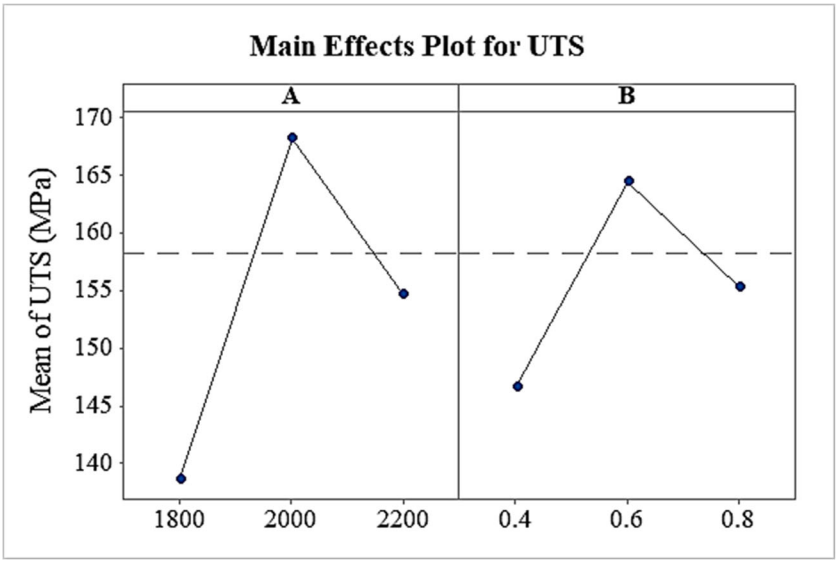

Fig. 8 Main effects plot for ultimate tensile strength (UTS) vs. factors (A=tool rotational speed in rpm, B=weld speed in rpm)

the pre-mid-region of the levels considered. A maximum yield strength of 145 MPa is achieved around the mid-level region.

4.3 Influence of process parameters on percentage elongation

Figure 12 shows the main effects plot between process parameters and percentage elongation. The increase in tool rotational speed and weld speed until the mid-level increases the percentage elongation. After which a similar increase decreases the percentage elongation. Equation 4 describes the nature of the contribution of process parameters for percentage elongation of the weld joint. The interactive effect of tool rotational speed and weld speed on the percentage elongation is shown in Fig. 13. The maximum value of the percentage elongation (8%) is obtained, while the welding is performed using mid-level of the process parameters considered ($x = 2000$ rpm, $y = 0.6$ rpm).

4.4 Optimization using desirability function approach

The predicted responses (Table 8) are obtained using the RSM technique. Since the optimization objective is to maximize the responses, these predicted responses are weighted as 1 (since its maximization function), and individual desirability (di) is found using Eq. 7. After calculating the individual desirability,

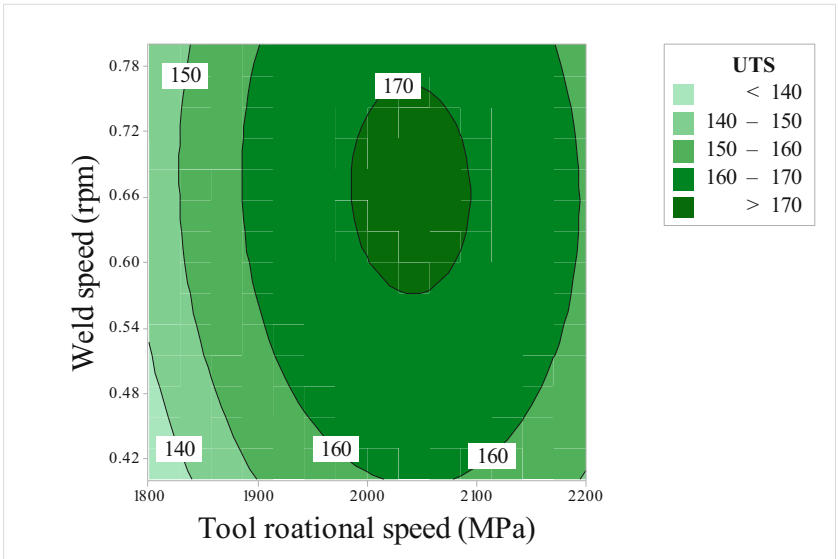

Fig. 9 Effect of weld speed and tool rotational speed on ultimate tensile strength

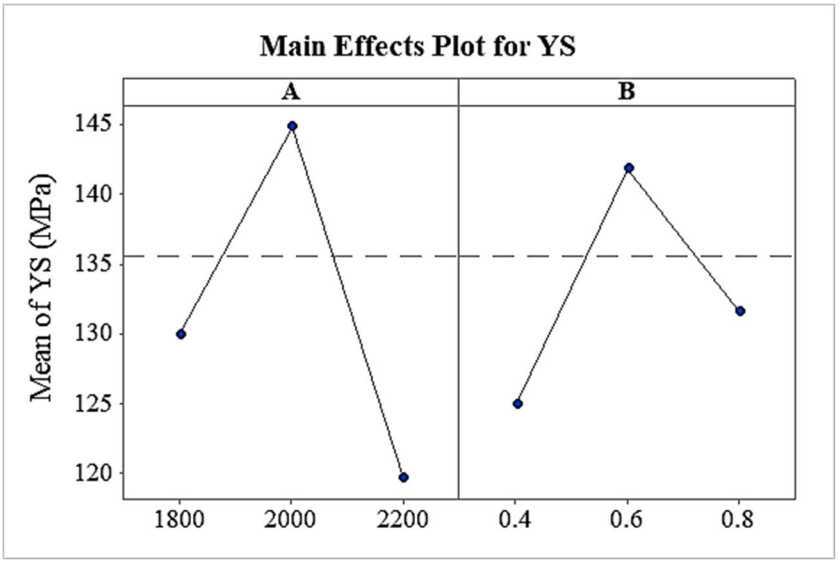

Fig. 10 Main effects plot for yield strength (YS) vs. factors (A=tool rotational speed in rpm, B=weld speed in rpm)

composite desirability (D) for each variable is arrived using Eq. 8. The composite desirability, along with rank for each operating condition, is tabulated in Table 9. From this table, it is clear that run no. 1 (A = 2000 rpm, B = 0.6 rpm) ranks 1 for having produced the optimal responses among all other available combinations (Ramanujam et al. 2014).

Furthermore, the developed model using the desirability function is used to the near-optimal solution rather than the available combinations (Mohapatra et al. 2019). The final optimal result is given in Fig. 14. Even though the available optimal parameters (run 1) is producing maximum responses, the multi-response prediction made by the desirability function suggests a still more optimal parameter condition of tool rotational speed of 1986 rpm and weld speed of 0.65 rpm. This parameter combination yields a maximum response value in yield strength of 148 MPa, an ultimate tensile strength of 170 MPa, and % elongation of 8.1 (Table 10).

5 Confirmation experiments

Even though the predicted parameter conditions are well below the allowable error limits when compared with the available parameter conditions, confirmation experiments are conducted for the predicted parameter values. A small modification was made in the fixture to deliver a welding speed of 0.65 rpm. A total of three runs were performed, and the average specimens are presented in Table 11. The predicted optimal parameters of tool rotational speed 1986 rpm, weld speed 0.65 rpm, and taper cylindrical tool pin profile produced joints

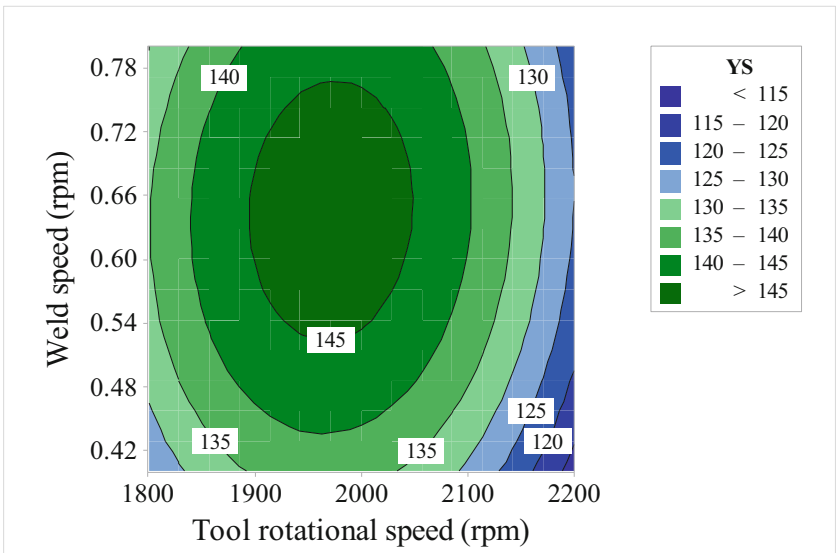

Fig. 11 Effect of weld speed and tool rotational speed on yield strength

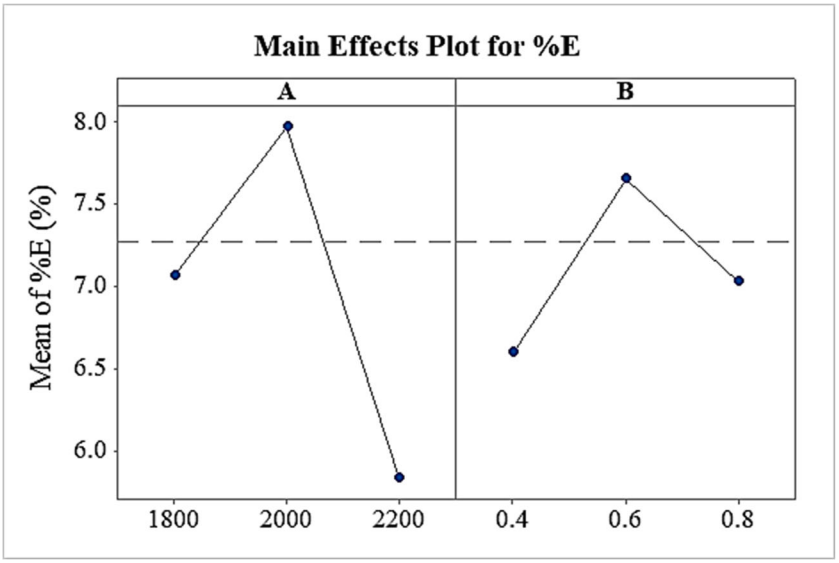

Fig. 12 Main effects plot for % elongation (%E) vs. factors (A=tool rotational speed in rpm, B=weld speed in rpm)

gave an ultimate tensile strength of 167 MPa, which has an error score of 1% (< confidence level of 95%). Also, the evaluated values of yield strength and percentage elongation are found to be optimal under the confidence level.

The sample obtained from the confirmation experiment number 3 is used for metallurgical study as it has very little error overall. The weld obtained using optimized parameters is then put forth for microstructural examination to infer the microstructural enhancement rendering to high-performance characteristics. Figure 15 shows the microstructure image of the optimized weld. The HAZ has less distorted grains with a linear flow pattern to the base metal. The TMAZ is characterized by elongated grains with a high degree of distortion. The stir zone has a fine-grained structure increasing the boundaries thus resulting in superior mechanical properties (Agrawal et al. 2017). There is a clear transition from heat affected zone (HAZ) to thermo-mechanically affected zone (TMAZ) and to stir zone (SZ), a typical grain transition behavior for FSWed AA6063-T6 (Moreira et al. 2008).

6 Conclusion

In this study, AA6063-T6 pipes have been joined using the FSW process. A multi-objective optimization model has been developed to optimize the process parameters, viz., tool rotational speed and weld speed, for maximizing the tensile properties of friction stir-welded pipes. The indigenously fabricated rotary fixture has been employed to facilitate the process of FSW of pipes. RSM has been used to predict the responses and develop the regression model. The developed regression

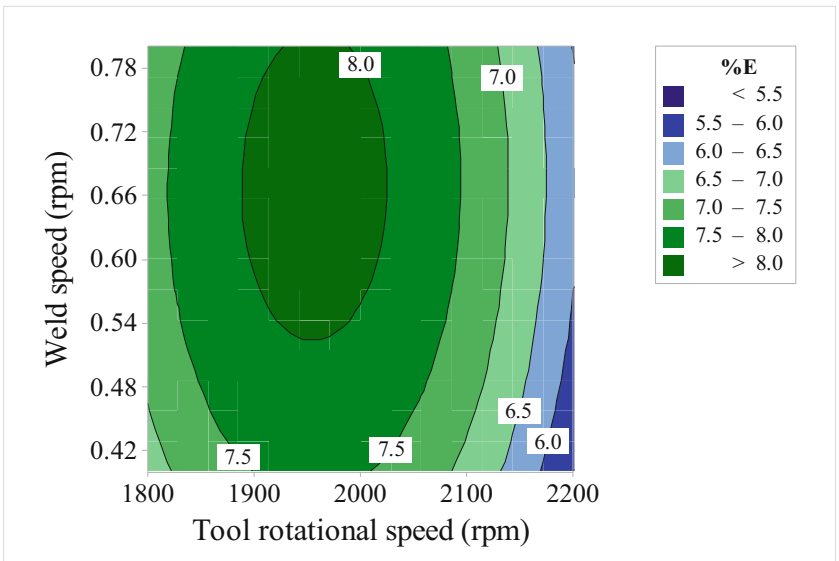

Fig. 13 Effect of weld speed and tool rotational speed on % elongation

Table 9 Evaluated results of desirability function

Run order	Predicted values			Individual desirability after weighted (d)			Composite desirability	
	YS (MPa)	UTS (MPa)	%E (%)	YS	UTS	%E	D	Rank
1	146.83	169.90	8.06	1.00000	1.00000	1.00000	1.0000	1
2	121.95	155.95	5.97	0.23246	0.66459	0.17818	0.3019	7
3	129.78	141.95	7.16	0.53604	0.25019	0.65808	0.4452	5
7	124.26	158.76	6.04	0.33723	0.71147	0.21302	0.3711	6
8	112.78	149.29	5.49	0.03677	0.44030	0.00957	0.0537	9
9	136.60	159.43	7.54	0.69954	0.72883	0.79668	0.7406	3
11	143.26	168.09	7.97	0.89523	0.95312	0.96529	0.9374	2
12	134.60	142.76	7.27	0.64080	0.29707	0.69292	0.509	4
13	125.62	131.29	6.77	0.34034	0.02590	0.48947	0.1628	8

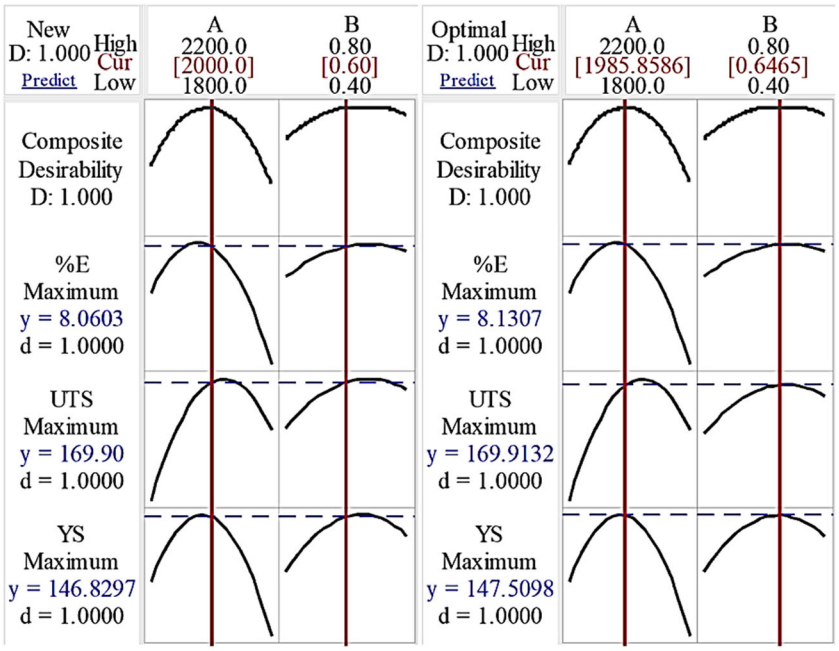

Fig. 14 Predicted responses for available (new) and optimal parameter conditions using desirability function

model has been evaluated using ANOVA. Based on this study, the following inferences are made:

i. The regression model developed for predicting the yield strength, ultimate tensile strength, and % of elongation of

Table 10 Optimized value for responses

Process parameters			Responses		
Process condition	Tool rotational speed (rpm)	Weld speed (rpm)	Yield strength (MPa)	Ultimate tensile strength (MPa)	% elongation %
Available	2000	0.6	146.83	169.90	8.06
Predicted	1986	0.65	147.51	169.91	8.13
% Improvement in responses			0.46	0.01	0.86

Table 11 Comparison of confirmation test with the results

Exp no.	Yield strength (MPa)			Ultimate tensile strength (MPa)			% elongation (%)		
	Obtained	Predicted	Error	Obtained	Predicted	Error	Obtained	Predicted	Error
1	144	148	2.7%	174	170	2.4%	8.4	8.1	3.7%
2	151	148	2.0%	175	170	2.9%	7.8	8.1	3.7%
3	145	148	2.0%	167	170	1.8%	8.3	8.1	2.5%

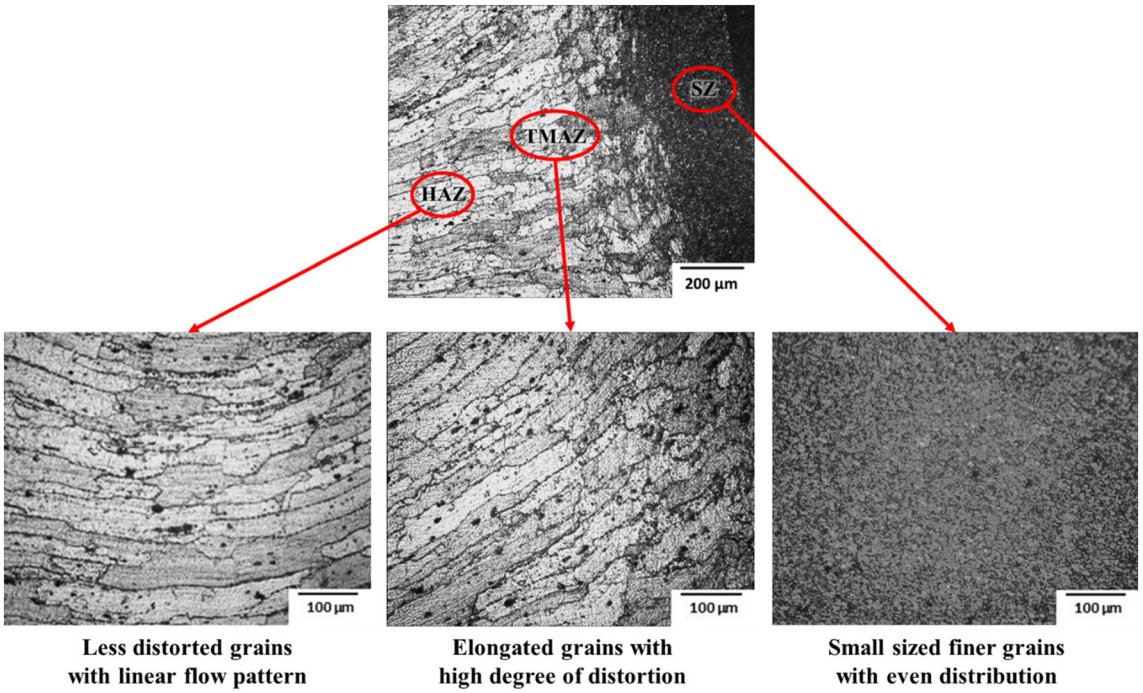

Fig. 15 The microstructure of various zones in the optimized weld of AA6063 T6 pipe joint

the pipe weld has good adequacy in delivering the responses above 95% confidence level.

ii. Tool rotational speed and weld speed offer equal influence over the tensile characteristics of the weld. Increase

Table 12 Predicted results as per the software output

Std order	Run order	Pt type	Blocks	A	B	YS	UTS	%E
11	1	0	1	2000	0.6	146.83	169.9	8.06
4	2	1	1	2200	0.8	121.95	155.95	5.97
3	3	1	1	1800	0.8	129.78	141.95	7.16
12	4	0	1	2000	0.6	146.83	169.9	8.06
13	5	0	1	2000	0.6	146.83	169.9	8.06
9	6	0	1	2000	0.6	146.83	169.9	8.06
6	7	−1	1	2200	0.6	124.26	158.76	6.04
2	8	1	1	2200	0.4	112.78	149.29	5.49
7	9	−1	1	2000	0.4	136.6	159.43	7.54
10	10	0	1	2000	0.6	146.83	169.9	8.06
8	11	−1	1	2000	0.8	143.26	168.09	7.97
5	12	-1	1	1800	0.6	134.6	142.76	7.27
1	13	1	1	1800	0.4	125.62	131.29	6.77

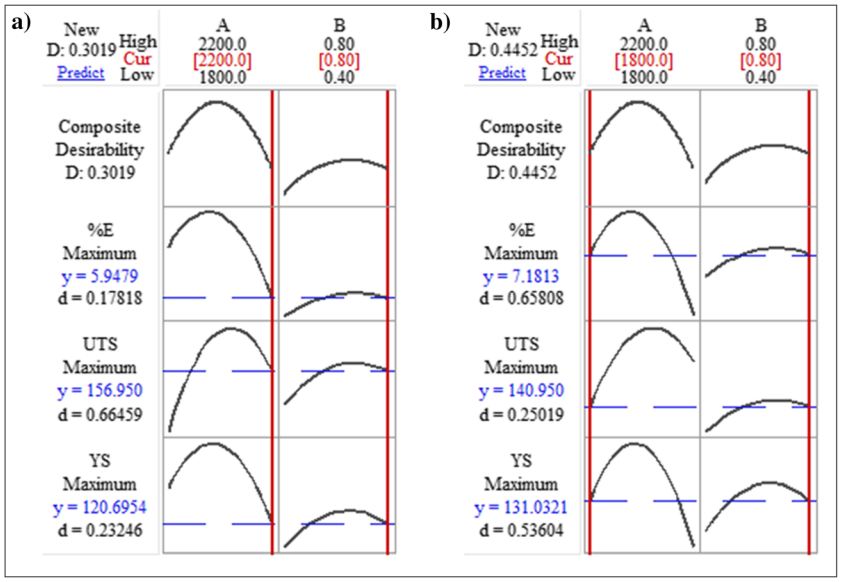

Fig. 16 Desirability calculations for run 2 and run 3

tool rotational speed or decrease in weld speed generates more heat, which has a more significant effect over the mechanical properties of the weld joint.

iii. The desirability function used in the study has predicted the optimal process parameter with a tool rotational speed of 1986 rpm and a welding speed of 0.65 rpm under considered operating conditions.

iv. Tool rotational speed of 1986 rpm and weld speed 0.65 rpm has produced weld joints having tensile properties superior having yield strength of 145 MPa, an ultimate tensile strength of 167 MPa and % elongation of 8.3, under considered operating conditions.

As the FSW process sooner or later will hit the commercial markets due to its mechanical and economic advantages over other processes, the results of this study will help make this process one step closer to this target. When the fixture developed in this present study is integrated to a machine tool, it will form a dedicated machine to carry out FSW process in pipes. This integration will enable a proportional control over the process parameters. This dependability between process parameters can further reduce the design variables. The study can be extended further by studying the combined effect of other process parameters over the weld joint quality. Also, other optimization techniques can be employed to compare the quality of prediction.

7 Replication of results

The results presented in this paper can be replicated using software like Minitab and Design–Expert (authors have used an academic version of Minitab 18), which have readymade tools for implementing RSM and desirability function.

7.1 The arrival of design matrix

The design matrix, presented in Table 4, is generated using a central composite design having a model as follows:

Central composite design			
Design summary			
Factors	2	Replicates	1
Base runs	13	Total runs	13
Base blocks	1	Total blocks	1
$\alpha = 1$			
Two-level factorial: full factorial			
Point types			
Cube points	4		
Center points in cube	5		
Axial points	4		
Center points in axial	0		

7.2 Obtaining the predicted responses

The experimental results are fed to the software, and the predicted results are populated. Table 12 shows the predicted results for the corresponding run order (the actual output of the software).

7.3 Application of desirability function

Figure 16 shows the sample desirability outputs for individual runs 2 and 3 (Cur values), obtained using the response optimizer option in the software.

Compliance with ethical standards

Conflict of interest The authors declare that they have no conflict of interest.

References

Agrawal AK, Narayanan RG, Kailas SV (2017) End forming behaviour of friction stir processed Al 6063-T6 tubes at different tool rotational speeds. J Strain Anal Eng Design 52:434–449

Arbegast WJ (2003) Modeling friction stir joining as a metalworking process Proceedings of Hot Deformation of Aluminum Alloys III: 313–327

Aydin H, Bayram A, Esme U, Kazancoglu Y, Guven O (2010) Application of Grey relation analysis (GRA) and Taguchi method for the parametric optimization of friction stir welding (FSW) process. Mater Technol 44:205–211

Babu KK, Panneerselvam K, Sathiya P, Haq AN, Sundarrajan S, Mastanaiah P, Murthy CS (2017) Parameter optimization of friction stir welding of cryorolled AA2219 alloy using artificial neural network modeling with genetic algorithm. Int J Adv Manuf Technol:1–13

Bayazid S, Farhangi H, Ghahramani A (2015) Investigation of friction stir welding parameters of 6063-7075 aluminum alloys by Taguchi method. Procedia Mater Sci 11:6–11

Chouhan D, Pal SK, Garg S (2013) Experimental study on the effect of welding parameters and tool pin profiles on mechanical properties of the FSW joints. Dimensions 806:28

Commin L, Dumont M, Masse J-E, Barrallier L (2009) Friction stir welding of AZ31 magnesium alloy rolled sheets: influence of processing parameters. Acta Mater 57:326–334

Derringer G, Suich R (1980) Simultaneous optimization of several response variables. J Qual Technol 12:214–219

Doos QM (2012) Bashar, Abdul wahab Experimental study of friction stir welding of 6061-T6 aluminium pipe. Int J Mech Eng Robot 1

Elangovan K, Balasubramanian V (2007) Influences of pin profile and rotational speed of the tool on the formation of friction stir processing zone in AA2219 aluminium alloy. Mater Sci Eng A 459:7–18

Elangovan K, Balasubramanian V (2008) Influences of tool pin profile and welding speed on the formation of friction stir processing zone in AA2219 aluminium alloy. J Mater Process Technol 200:163–175

Gadakh VS, Adepu K (2013) Heat generation model for taper cylindrical pin profile in FSW. J Mater Res Technol 2:370–375

Ganapathy T, Lenin K, Pannerselvam K (2017) Process parameters optimization of friction stir welding in aluminium alloy 6063-T6 by Taguchi Method. In: Applied Mechanics and Materials. Trans Tech Publ, pp 97–104

Ghaffarpour M, Aziz A, Hejazi T-H (2017) Optimization of friction stir welding parameters using multiple response surface methodology. Proceedings of the Institution of Mechanical Engineers Part L: Journal of Materials: Design and Applications 231:571–583

Gupta SK, Pandey K, Kumar R (2018) Multi-objective optimization of friction stir welding process parameters for joining of dissimilar AA5083/AA6063 aluminum alloys using hybrid approach. Proceedings of the Institution of Mechanical Engineers, Part L: Journal of Materials: Design and Applications 232:343353

Ismail A, Awang M, Fawad H, Ahmad K (2013) Friction stir welding on aluminum alloy 6063 pipe. In: Proceedings of the 7th Asia Pacific IIW International Congress, Singapore. pp 78–81

Kadaganchi R, Gankidi MR, Gokhale H (2015) Optimization of process parameters of aluminum alloy AA 2014-T6 friction stir welds by response surface methodology. Defence Technology 11:209–219

Kalavathy MH, Regupathi I, Pillai MG, Miranda LR (2009) Modelling, analysis and optimization of adsorption parameters for H3PO4 activated rubber wood sawdust using response surface methodology (RSM) colloids and surfaces B: biointerfaces 70:35-45. https://doi.org/10.1016/j.colsurfb.2008.12.007

Khourshid A, Sabry I (2013) Friction stir welding study on aluminum pipe. Int J Mech Eng Robot Res 2:331–339

Lammlein D, Gibson B, DeLapp D, Cox C, Strauss A, Cook G (2012) The friction stir welding of small-diameter pipe: an experimental and numerical proof of concept for automation and manufacturing. Proc Inst Mech Eng B J Eng Manuf 226:383–398

Mallieswaran K, Padmanabhan R, Balasubramanian V (2018) Friction stir welding parameters optimization for tailored welded blank sheets of AA1100 with AA6061 dissimilar alloy using response surface methodology. Advance Mater Proces Technol:1–16

Mehta KP, Badheka VJ (2016) Effects of tilt angle on the properties of dissimilar friction stir welding copper to aluminum Materials and Manufacturing processes 31:255–263

Mohapatra T, Sahoo SS, Padhi BN (2019) Analysis, prediction and multi-response optimization of heat transfer characteristics of a three fluid heat exchanger using response surface methodology and desirability function approach. Appl Therm Eng 151:536–555. https://doi.org/10.1016/j.applthermaleng.2019.02.001

Moreira P, De Oliveira F, De Castro P (2008) Fatigue behaviour of notched specimens of friction stir welded aluminium alloy 6063-T6. J Mater Process Technol 207:283–292

Myers RH, Montgomery DC, Anderson-Cook CM (2016) Response surface methodology: process and product optimization using designed experiments. John Wiley & Sons

Padmanaban G, Balasubramanian V (2009) Selection of FSW tool pin profile, shoulder diameter and material for joining AZ31B magnesium alloy–an experimental approach. Mater Des 30:2647–2656

Pandiyarajan R, Maran P, Murugan N, Marimuthu S, Sornakumar T (2019) Friction stir welding of hybrid AA 6061-ZrO2-C composites FSW process optimization using desirability approach. Mater Res Express 6:066553

Ramanujam R, Maiyar LM, KVM V (2014) Multi response optimization using ANOVA and desirability function analysis: a case study in end milling of Inconel alloy. ARPN J Eng Appl Sci 9:457–463

Sahu PK, Kumari K, Pal S, Pal SK (2016) Hybrid fuzzy-grey-Taguchi based multi weld quality optimization of Al/Cu dissimilar friction stir welded joints. Adv Manuf 4:237–247

Sashank JS, Sampath P, Krishna PS, Sagar R, Venukumar S, Muthukumaran S (2018) Effects of friction stir welding on microstructure and mechanical properties of 6063 aluminium alloy. Materials Today: Proceedings 5:8348–8353

Selaimia A-A, Yallese MA, Bensouilah H, Meddour I, Khattabi R, Mabrouki T (2017) Modeling and optimization in dry face milling of X2CrNi18-9 austenitic stainless steel using RMS and desirability approach. Measurement 107:53–67. https://doi.org/10.1016/j.measurement.2017.05.012

Srivastava M, Maheshwari S, Kundra TK, Rathee S (2017) Multi-response optimization of fused deposition modelling process parameters of ABS using response surface methodology (RSM)-based desirability analysis materials today: Proceedings 4:1972-1977 https://doi.org/10.1016/j.matpr.2017.02.043

Su H, Wu C, Pittner A, Rethmeier M (2013) Simultaneous measurement of tool torque, traverse force and axial force in friction stir welding. J Manuf Process 15:495–500

Sudhagar S, Sakthivel M, Mathew PJ, Daniel SAA (2017) A multi criteria decision making approach for process improvement in friction stir welding of aluminium alloy. Measurement 108:1–8

Verma S, Gupta M, Misra JP (2018) Optimization of process parameters in friction stir welding of armor-marine grade aluminium alloy using desirability approach. Mater Res Express 6:026505. https://doi.org/10.1088/2053-1591/aaea01

Vijay S, Murugan N (2010) Influence of tool pin profile on the metallurgical and mechanical properties of friction stir welded Al–10wt.% TiB 2 metal matrix composite. Mater Des 31:3585–3589

Wakchaure K, Thakur A, Gadakh V, Kumar A (2018) Multi-objective optimization of friction stir welding of Aluminium alloy 6082-T6 using hybrid Taguchi-Grey relation analysis-ANN. Method Materials Today: Proceedings 5:7150–7159

Wang F, Li W, Shen J, Hu S, dos Santos J (2015) Effect of tool rotational speed on the microstructure and mechanical properties of bobbin tool friction stir welding of Al–Li alloy. Mater Des 86:933–940